

Combined spectroscopic and molecular docking study of binding interaction of pyrano [3, 2-f] quinoline derivatives with bovine serum albumins and its application in mammalian cell imaging

Swarup Roy¹, Sudipta ponra², Tapas Ghosh², Ratan Sadhukhan¹, K. C. Majumdar^{2*}, Tapan Kumar Das^{1*}

¹Department of Biochemistry and Biophysics, University of Kalyani, Kalyani 741235, West Bengal, India

²Departments of Chemistry, University of Kalyani, Kalyani 741235, West Bengal, India

*Corresponding author. Tel: (+91) 34-73238373; E-mail: tapankumardas175@gmail.com (T.K. Das); Tel: (+91) 33-2582 7521; E-mail: kcmklyuniv@gmail.com (K.C. Majumdar)

Received: 06 April 2015, Revised: 12 June 2015 and Accepted: 26 June 2015

ABSTRACT

The interaction between pyrano [3, 2-f] quinoline derivatives (TPQ) and bovine serum albumin (BSA) was studied using spectroscopic techniques. The TPQ quench the fluorescence of BSA through dynamic quenching. According to Van't Hoff equation, the thermodynamic parameters were calculated and which indicated hydrogen bonds and van der Waals forces played a prime role in stabilizing the BSA-TPQ complexes. Also, the average binding distance (r) and the critical energy transfer distance (R_0) between TPQ and BSA were also evaluated according to Förster's non-radiative energy transfer (FRET) theory. What is more, UV-visible and circular dichroism results showed that the addition of TPQ changed the secondary structure of BSA and led to a reduction in content α -helix (%) content. It was also observed that TPQ shows cell staining property to the cultured HeLa cell line. Theoretical docking study of interaction between BSA and TPQ also supported the experimental results. All the results suggested that BSA experienced substantial conformational changes induced by TPQ; this may be useful to study synthetic organic molecules for their application as pharmaceuticals. Copyright © 2015 VBRI Press.

Keywords: Bovine serum albumin; TPQ; docking; spectroscopic method; cell staining.

Introduction

Serum albumins, the most abundant and major soluble protein constituent present in the blood stream of vertebrates. These serve as a transport carrier of drugs due to their greater ability to bind reversibly with a large variety of endogenous and exogenous ligands present in blood [1]. Serum albumins including human serum albumin (HSA) and bovine serum albumin (BSA) possess numerous functionalities. Both BSA and HSA are 66 kDa globular proteins. They consist of amino acid chains forming a single polypeptide with well-known sequence. They contain three homologous α -helix domains (I-III) assembled to form heart shaped molecules [2-4]. Due to the medical importance, low cost, ready availability, unusual ligand-binding capacity and intrinsic fluorescence properties BSA was selected as a protein model [5, 6].

Quinoline and its derivatives are found to have broad applications in drug development, material science, [7-10] bio-organometallic processes, [11] and agrochemicals and

effect chemicals such as dyestuffs, corrosion inhibitors, and in medicinal chemistry [12]. Furthermore, substituted quinolines also exhibit numerous biological activities as antagonists of endothelin [13], 5HT₃ [14], and NK-3 receptors [15] and also function as inhibitors of gastric (H⁺/K⁺)-ATP-ase [16] and dihydroorotate dehydrogenase [17]. In precise, pyrano [3, 2-f] quinolines show several unique biological activities, such as psychotropic, [18] antiallergic [19], anti-inflammatory [20], and estrogenic [21] activities and are used as potential pharmaceuticals [22]. Helietidine, dutadrupine, and geibalansine [23-26] are among some of the examples of natural products containing pyranoquinoline as core structure. As a result of the aforesaid significance of these scaffolds in drug discovery and medicinal chemistry, efficient synthesis and further biological testing's of pyranoquinoline derivatives remains a centre of attraction to many synthetic chemists including us.

The aim of the present work was to determine the affinity of TPQ to BSA, and to investigate the

thermodynamics of their interaction. We planned to investigate the binding of TPQ to BSA by using fluorescence, circular dichroism and UV-Vis absorption spectral studies and by docking methods. We also, desired to investigate the cell staining property of TPQ to the cultured HeLa cell line. This study may provide valuable information related the biological effects of TPQ and therapeutic effect of this drug in pharmacology and pharmacodynamics.

Experimental

Materials

The pyrano [3, 2-*f*] quinoline derivatives required for our study was prepared according to published procedure [27] as shown in **scheme 1** (in the supporting information). The interesting feature of these compounds is the appearance of emission peaks in the range of 500-520 nm. The emission peak appeared in the range of 500-520 nm is generally due to coumarin motifs. **Fig. S1** shows the emission spectra of five compounds upon excitation at 450 nm.

Bovine Serum Albumin (Sigma) was used in this experiment. The stock solution of BSA was prepared by dissolving BSA in a Tris-HCl (50 mM, pH 7.4) buffer to make the concentration as 1 μ M. TPQ (1 mM) in methanol. All the media, fetal bovine serum, antibiotics for cell culture were purchased from HiMedia, India. Other fine chemicals and fluorescent dye Hoechst were purchased from SRL India, Sigma Aldrich. All the other chemicals were of analytical reagent grade and double distilled water was used throughout the experimental work.

Apparatus

Fluorescence spectra were recorded on agilent technologies Cary-Eclipse fluorescence spectrophotometer well-equipped with Cary temperature controller. The absorption spectra were obtained from a Cary 100 UV-VIS Spectrophotometer (Agilent Technologies). Circular dichroism spectra were recorded on a Jasco J-815 CD spectrometer. All the images were taken using a Carl Zeiss Axio vision 2 fluorescence microscope.

Methods

UV-Visible spectroscopy: The absorption titration experiments were performed by keeping the concentration of BSA 1 μ M while varying the TPQ concentration (0 to 30 μ M). The absorption spectra were recorded from 230 to 330 nm at room temperature (303 K). All the experiments were performed in Tris-HCl (50 mM, pH 7.4) buffer in a conventional quartz cell.

Intrinsic fluorescence: Bovine serum albumin solution (1 μ M) was titrated by successive additions of (0 to 20 μ M) TPQ. Fluorescence spectra were measured in the range of 300-450 nm at the excitation wavelength of 280 nm. The fluorescence spectra were performed at four temperatures (293, 300, 308 and 315 K). The range of synchronous scanning were $\lambda_{ex} = 240$, $\lambda_{em} (a) = 255$, $\lambda_{em} (b) = 300$ nm, where the differences in the wavelengths ($\Delta\lambda$) were 15 and 60 nm.

Circular dichroism (CD) spectra: The far-UV CD region (190-260), which corresponds to peptide bond absorption, was analyzed to give the content of the regular secondary structure in BSA. Protein solutions were prepared in Tris-HCl (50 mM, pH 7.4) buffer. BSA solution of 0.04 μ M was used to obtain the spectra and spectral changes of BSA were monitored after adding TPQ (0 to 50 μ M).

Cell culture: Human cervical cancer cell line HeLa was obtained from National Centre for Cell Sciences, Pune, India. HeLa cells were grown in DMEM supplemented with 10 % fetal bovine serum (complete medium) at 37 °C in humidified atmosphere containing 5 % CO₂.

Cell staining with the compounds: The cells were processed for staining following previous protocol with slight modification [28]. The HeLa cells were grown over cover slip for 24 h and washed thrice with PBS to remove the medium. The cells over the cover slip were fixed with methanol-acetone (1:1) at 4 °C for 1 h. The cover slip was washed twice with PBS and incubated with 1 mM TPQ in PBS for 10 min in dark. After washing with PBS the cover slip was placed upside down over the glass slide so that the cells touched the glass slide. Then the slides were observed under fluorescence microscope with UV excitation as well as in normal light mode [29-31].

Molecular modeling: The crystal structure of BSA was obtained from the protein data bank (entry code 4F5S). The Auto dock 4.0 was employed to compute the possible binding mode of TPQ with BSA. The 3-D structure of TPQ and BSA was modeled using molecular modeling software discovery digital studio 4.0. The docking calculations were performed using the Lamarckian genetic algorithm (LGA) for ligand conformational searching. To compute the possible binding conformations of TPQ, LGA applied in the Auto dock 4.0. During the docking process, a maximum of 10 different conformations were considered for TPQ. The conformer with the lowest binding free energy was used for further analysis.

Results and discussion

Absorption spectra

UV-Vis absorption spectrum is a very simple and useful technique to know the structural change and detecting the complex formation [32]. The absorption spectra of BSA in the presence of TPQ were recorded and presented in **Fig. 1**. As presented in Fig, with the addition of TPQ the absorbance intensity of BSA was increased and the absorption spectra maximum was shifted towards shorter wavelength region, which suggests that BSA may bind to TPQ and form the complex.

The values of the association constant (K_{app}) were estimated on the basis of Benesi and Hildebrand equation, from the BSA-TPQ absorption spectra according to the previously described methods [33]. The K_{app} is calculated using following equation 1 [34].

$$\frac{1}{A_{obs} - A_0} = \frac{1}{A_c - A_0} + \frac{1}{K_{app}(A_c - A_0)[TPQ]} \quad (1)$$

Here, A_0 is the absorbance of BSA in the absence of TPQ and A_C is the recorded absorbance for BSA at different TPQ concentrations. The double reciprocal plot of $1/(A_{\text{obs}}-A_0)$ vs $1/[\text{TPQ}]$ is linear and K_{app} was estimated to be 3.05×10^3 L/mol in case of TPQ 2 ($R=0.9984$, where R is the correlation coefficient) [Fig. 1 inset] [35]. In case of TPQ 3, TPQ 4, TPQ 5 and TPQ 9; K_{app} values are 1.96×10^4 , 1.37×10^4 , 6.89×10^3 , and 6.01×10^3 L/mol respectively, results were shown in S1, given in supplementary file ($R=0.9936$, 0.9992 , 0.9987 , and 0.9988 for TPQ 3, TPQ 4, TPQ 5 and TPQ 9 respectively). The value of K_{app} is small, thereby indicating formation of a weak complex between BSA and TPQ. The above results indicate that in case of TPQ 3, K_{app} value is highest and is lowest in case of TPQ 2.

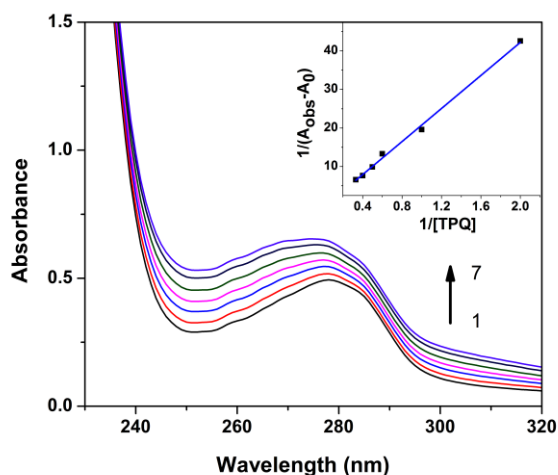


Fig. 1. Absorption spectra of BSA (1 μM) in presence of TPQ 2 (1-7): (0, 5, 10, 15, 20, 25, and 30 μM), inset showing calculation of K_{app} of BSA-TPQ 2 complex; $1/(A_{\text{obs}}-A_0)$ vs. $1/[\text{TPQ}]$ plot.

The fluorescence quenching spectra

BSA has a strong fluorescence emission when excited at 279 nm wavelength. **Fig. 2** shows the emission spectra of BSA in the presence of different concentrations of TPQ. It was observed that the fluorescence intensity of BSA sharply decreased with the increasing concentration of TPQ. These data indicated that TPQ can interact with BSA and quench intensity of fluorescence.

The fluorescence quenching mechanism

A variety of molecular interactions results in quenching, including excited-state reactions, molecular rearrangements, energy transfer, ground-state complex formation, and collisional quenching [35]. The possible quenching mechanism can be represented by the Stern-Volmer equation [36, 37].

$$F_0 / F = 1 + K_q \tau_0 [Q] = 1 + K_{sv} [Q] \quad (2)$$

where, F_0 and F denote the fluorescence intensities in the absence and presence of quencher, respectively. K_q is the bimolecular quenching rate constant; τ_0 is the average life time of the molecule without the quencher which is about 10^{-8} s. K_{sv} is Stern-Volmer quenching constant; $[Q]$ is the concentration of the quencher [38-40]. The values of K_{sv}

decreases with increasing temperature for static quenching and increases for dynamic quenching.

The Stern-Volmer plots of the quenching of BSA fluorescence separately by TPQ at different temperatures are presented in **Fig. 2** inset. The calculated results are mentioned in **Table 1** (Supplementary information). In case of dynamic quenching it is known that the maximum scatter quenching collision constant of various quenchers with the biomolecule is approximately 1×10^{10} L/mol/s. The experimental quenching constant was found to increase gradually with increase of temperature. This indicates that in all five cases of quenching mechanism is a dynamic quenching process [40, 41]. From **Table 1**, it is observed that the binding constants of the interaction between TPQ and BSA increases in the following order: TPQ 5 < TPQ 9 < TPQ 3 < TPQ 2 < TPQ 4 which indicates that the compound TPQ 4 has the strongest ability to quench BSA fluorescence and compound TPQ 5 has the weakest ability to quench BSA.

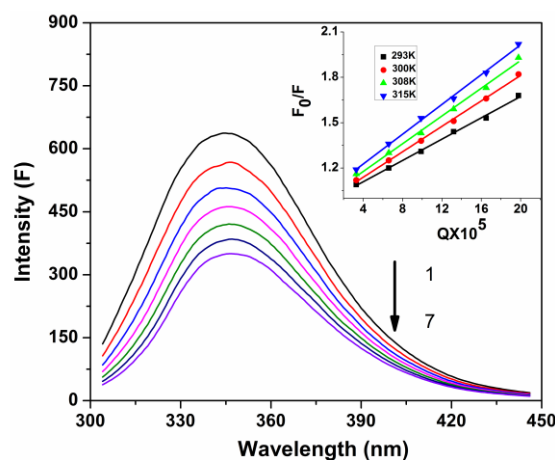


Fig. 2. Fluorescence quenching spectra of BSA by TPQ 2, $\lambda_{\text{exc}}=279$ nm; C (BSA) = $1 \mu\text{M}$; C (TPQ 2) (1-7): (0, 3.3, 6.6, 9.9, 13.2, 16.5 and 19.8 μM respectively), inset showing Stern Volmer plot for TPQ 2 and BSA at 293, 300, 308, and 315 K respectively.

Binding constant (K) and number of binding sites (n)

When small molecules interact independently with a set of equivalent sites on a biomolecule, the equilibrium between biomolecule and small molecule is expressed by Eq.3. The number of binding sites (n) and binding constant (K) of interaction between TPQ and BSA can be calculated by using the same equation [42].

$$\log \frac{F_0 - F}{F} = \log K + n \log [Q] \quad (3)$$

A plot of $\log [(F_0-F)/F]$ vs $\log [Q]$ makes a straight line, whose slope represents n (the number of binding sites between TPQ and BSA) and the length of intercept on Y-axis is $\log K$.

Fig. 3 denotes the double logarithm plots and **Table 2** gives the corresponding results. The values of ' n ' at the experimental temperatures were approximately equal to one which designate that there is a single binding site in BSA separately for TPQ and which is dependent on temperature ranging from 293 to 315 K.

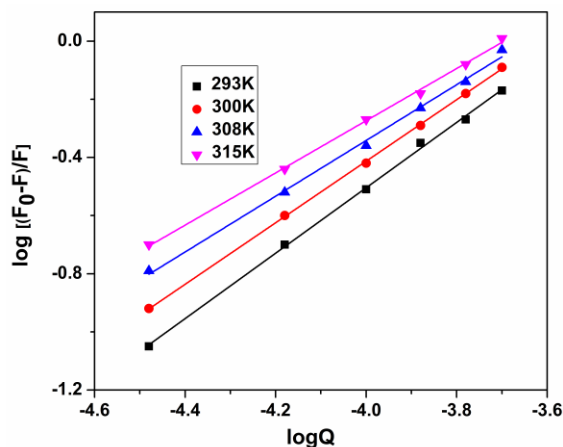


Fig. 3. Plots of TPQ 2 quenching effect on BSA fluorescence at varying temperature (293, 300, 308, and 315 K).

Table 2. Binding constants (K) and number of binding sites (n) of BSA by TPQ at varying temperatures.

Compound	Temperature(K)	K (L/mol)	n	R ^a
TPQ2	293	15.8×10 ⁸	1.12	0.9993
TPQ3	293	6.76×10 ⁷	0.95	0.9991
TPQ4	293	30.9×10 ⁸	1.12	0.9988
TPQ5	293	28.2×10 ⁷	0.90	0.9962
TPQ9	293	19.4×10 ⁸	1.02	0.9994
TPQ2	300	5.62×10 ⁸	1.06	0.9998
TPQ3	300	3.89×10 ⁷	0.94	0.9992
TPQ4	300	3.30×10 ⁸	1.00	0.9991
TPQ5	300	5.60×10 ⁷	0.80	0.9985
TPQ9	300	6.7×10 ⁸	1.01	0.9976
TPQ2	308	1.15×10 ⁸	0.96	0.9984
TPQ3	308	1.38×10 ⁷	0.84	0.9999
TPQ4	308	0.67×10 ⁸	0.93	0.9980
TPQ5	308	1.99×10 ⁷	0.73	0.9962
TPQ9	308	0.25×10 ⁸	0.92	0.9980
TPQ2	315	0.4×10 ⁸	0.90	0.9993
TPQ3	315	0.46×10 ⁷	0.78	0.9987
TPQ4	315	0.08×10 ⁸	0.80	0.9976
TPQ5	315	0.32×10 ⁷	0.58	0.9944
TPQ9	315	0.06×10 ⁸	0.83	0.9990

From **Table 2**, it is observed that the binding constants of the interaction between TPQ and BSA increases in the following order: TPQ 3 < TPQ 5 < TPQ 2 < TPQ 9 < TPQ 4 which indicates that the compound TPQ 4 has the strongest ability to bind with BSA and compound and TPQ 3 is the weakest. With increase of temperature the binding constant K decreases which indicates that the stability of the TPQ-BSA complexes becomes weaker with rise of temperature.

Thermodynamic parameters and nature of binding forces

The possible interaction forces between the biomolecule and small molecules are hydrogen bonding, van der Waals, hydrophobic and hydrophilic, and electrostatic interactions [43]. The thermodynamic parameters enthalpy change (ΔH) and entropy change (ΔS) can be determined using the Van't Hoff eq. (Eq. 4), where K is the binding constant at the corresponding temperature (Fig. 4).

$$\ln K = -\Delta H / RT + \Delta S / R \quad (4)$$

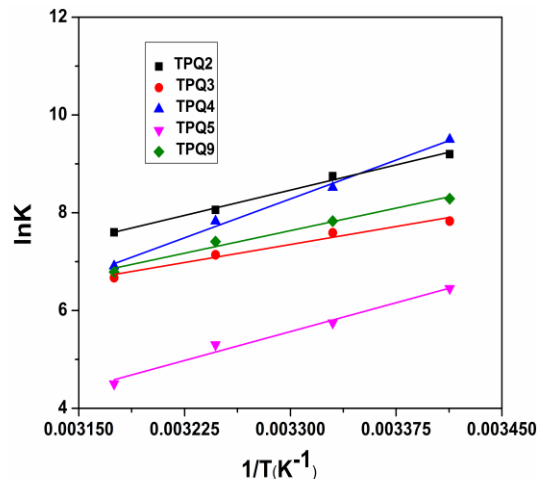


Fig. 4. The Van't Hoff plot for the interaction of BSA and TPQ.

ΔH and ΔS can be determined from the slope and intercept of linear Van't Hoff plots. The Gibbs free energy (ΔG) can be calculated from the equation 5.

$$\Delta G = \Delta H - T\Delta S = -RT \ln K \quad (5)$$

According to the enthalpy and entropy changes, the model of interaction between small molecule and biomolecules can be summarized as, $\Delta H > 0$ and $\Delta S > 0$ indicate hydrophobic forces; $\Delta H < 0$ and $\Delta S < 0$ indicate van der Waals interactions and hydrogen bonding; $\Delta H \approx 0$ and $\Delta S > 0$ indicate electrostatic interaction [43]. The values of thermodynamic parameters were mentioned in **Table 3**. As shown in **Table 3**, ΔG , ΔS and ΔH are found to be negative for TPQ-BSA complexes. Therefore, the formation of TPQ-BSA complexes is spontaneous and exothermic reaction follows a negative ΔS value. According to previous study [43-46], negative values of ΔS , and ΔH suggested that weak forces like van der Waals and hydrogen bonding were principal factor in this binding process. The negative value of ΔG suggests that the interaction process between the biomolecule and biologically active synthetic compound is spontaneous.

Synchronous fluorescence spectra

Synchronous fluorescence spectroscopy is used to analyze the micro-environmental changes of chromophores [47]. A synchronous fluorescence spectrum gives the information on the molecular environment of the fluorophores functional group. The value of $\Delta\lambda$ i.e. difference between excitation and emission wavelengths is an important operating parameter. According to Miller [48] when $\Delta\lambda = 15$ nm, synchronous fluorescence spectrum indicates the change in the microenvironment of tyrosine residues and when $\Delta\lambda = 60$ nm, it provides information on the microenvironment of tryptophan residues.

It can be seen from the **Fig. S2(b)** that for TPQ 2 when $\Delta\lambda = 60$ nm there is a blue shift in the emission wavelength of tryptophan. When $\Delta\lambda = 15$ nm, (**Fig. S2(a)**) there is a slight blue shift in emission wavelength of tyrosine. The blue shift in the emission maxima of **Fig. S2** indicates the polarity around the tyrosine and tryptophan residues is decreased and the hydrophobicity is increased in the

presence of TPQ [49]. These results suggest that TPQ induces a little conformational change in BSA. In case of TPQ 3, TPQ 4, TPQ 5 and TPQ 9 similar kind of results were observed (S1).

Table 3. Thermodynamic parameters for the binding of STP with BSA at different temperatures.

Compound	Temperature (K)	ΔH (kJ/mol)	ΔS (J/mol/K)	ΔG (kJ/mol)
TPQ2	293	-57.26	-118.64	-22.50
TPQ3	293	-40.81	-73.49	-19.28
TPQ4	293	-88.12	-221.90	-23.11
TPQ5	293	-65.48	-169.77	-15.74
TPQ9	293	-51.11	-105.17	-20.30
TPQ2	300			-21.67
TPQ3	300			-18.76
TPQ4	300			-21.55
TPQ5	300			-14.55
TPQ9	300			-19.38
TPQ2	308			-20.72
TPQ3	308			-18.18
TPQ4	308			-19.78
TPQ5	308			-13.19
TPQ9	308			-18.76
TPQ2	315			-19.89
TPQ3	315			-17.66
TPQ4	315			-18.23
TPQ5	315			-12.0
TPQ9	315			-17.98

Circular dichroism spectroscopy

Circular dichroism is commonly used to calculate the secondary structure of macromolecules [50]. The CD spectra of BSA showed two negative minima at 208 nm and 222 nm, which is typical characterization of the helix structure of this class of proteins [51]. **Fig. 6** presents the helicity of BSA in the presence of increasing concentration of TPQ.

In the wavelength region of 190–260 nm, the CD spectrum of a protein gives information about its conformation in relation to the secondary structure. The CD results were expressed in terms of mean residue ellipticity (MRE) in $\text{deg cm}^2 \text{dmol}^{-1}$ according to the following equation [32]:

$$MRE = \frac{\text{obsCD}(\text{mdeg})}{C_p \times n \times l \times 10} \quad (6)$$

where, C_p is the molar concentration of the protein, n is the number of amino acid residues and l is the path length. The α -helical contents of free and combined BSA were calculated from MRE values at 208 nm using the equation [52]:

$$\alpha\text{-helix}(\%) = \frac{-MRE_{208} - 4000}{33000 - 4000} \times 100 \quad (7)$$

where, MRE_{208} is the observed MRE value at 208 nm, 4000 is the MRE of the β -form and random coil conformation cross at 208 nm and 33000 is the MRE value of a pure α -helix at 208 nm. From the above equations (6-7), the helicity in the secondary structure of BSA can be calculated.

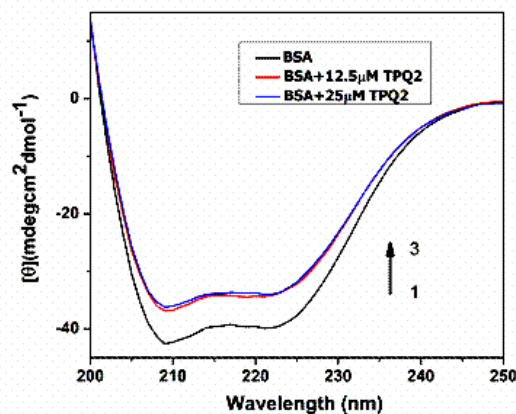


Fig. 6. UV-CD spectra of BSA (0.04 μM) in presence of TPQ 2 (0 to 25 μM)

According to the above equation the percentage of α -helix of BSA is computed and it shows that the percentage of helicity of BSA is 47.20 % in pure BSA. In presence of TPQ2, α -helix content decreases to 39.39 % and 38.40 % for 12.5 μM and 25 μM respectively. The data were indicative of the loss of α -helix content (8.8 %) due to the interaction of TPQ with BSA. The percentage of protein α -helix content decrease indicated that TPQ bound with the amino acid residue of the main polypeptide chain of BSA and destroyed their hydrogen bonding networks. This indicates that TPQ has altered the secondary structure of BSA [53]. The binding of TPQ 2 to BSA changes both these bands at 208 nm and 222 nm and it is apparent that interaction of TPQ 2 with BSA may cause some conformational change of the protein. In case of TPQ 3, TPQ 4, TPQ 5 and TPQ 9 respectively similar type of results were observed (S1).

Energy transfer

The importance of the energy transfer in biochemistry is that the efficiency of transfer can be used to evaluate the distance between the ligand and the tryptophan residues in the protein [54]. The overlap of the UV-Vis absorption spectrum of TPQ2 with the fluorescence emission spectrum of BSA is shown in **Fig. S3** (cf., supporting information).

According to FRET [55], the distance (r) of binding between TPQ and BSA, the efficiency E of energy transfer between the donor (biomolecule) and acceptor (small molecule), can be calculated using the following equation.

$$E = 1 - \frac{F}{F_0} = \frac{R_0^6}{(R_0^6 + r^6)} \quad (8)$$

$$R_0^6 = 8.8 \times 10^{-25} k^2 N^{-4} \phi J \quad (9)$$

In Eq. (8), E is the efficiency of transfer between the donor and the acceptor and R_0 is the critical distance when the efficiency of transfer is 50 %. F_0 and F mean the fluorescence intensity of amino acid in the absence and in the presence of quencher (TPQ), respectively [56]. In Eq. (9), K^2 is the spatial orientation factor of the dipole, N is the refractive index of the medium, ϕ is the fluorescence quantum yield of the donor. In this case, $K^2 = 2/3$, $N =$

1.336 and $\phi = 0.118$ [57]. J is the effect of the spectral overlap between the emission spectrum of the donor and the absorption spectrum of the acceptor and it can be obtained from the following equation:

$$J = \frac{\sum F(\lambda)\varepsilon(\lambda)\lambda^4\Delta\lambda}{\sum F(\lambda)\Delta\lambda} \quad (10)$$

In Eq. (10), $F(\lambda)$ is the fluorescence intensity of the fluorescence of the acceptor at wavelength λ . According to the above equation (Eq. 8-10) and experimental results we obtained for TPQ 2, $J = 2.82 \times 10^{-15} \text{ cm}^3 \times \text{L/mol}$, $E = 0.89$, $R_0 = 2.07 \text{ nm}$. From the Eq. (9), the value of $r = 2.93 \text{ nm}$ was obtained. In case of TPQ 3, TPQ 4, TPQ 5 and TPQ 9 also similar form of results were observed (S1, Given in supplementary file). The energy transfer results are shown in **Table 4**. The distance between donor molecule and acceptor molecule $r < 7$ for all individual of the five compounds of TPQ were observed, suggesting that the energy transfer process is a non-radiative type [58].

Cell staining with the complex

We have also investigated whether TPQ could be used to stain the cultured mammalian cells. Hoechst dye is a well-known DNA binding compound and hence the cells can be observed under fluorescence microscope with UV filter with excitation near 365 nm. The cell stained with Hoechst is shown in **Fig S4(F)** (Supporting information). We have tested the synthesized compound's staining ability of cultured cells as described in methods and observed that all the compounds are able to stain the cultured HeLa cells after fixing. The HeLa cells stained with compounds TPQ 2-5 and TPQ 9 are shown in **Fig. S4(B-E)**. Possibly, the compounds can bind the cellular protein components and thus making the cells visible under fluorescence microscope due to their intrinsic fluorescence. The cell image intensity for all the compounds as evident from the figures that compound TPQ 3 (**Fig S4**, supporting information) gave highest intensity. However, the fluorescence intensity for other complexes was observed to be less than that of our standard control. So, these complexes could be used as dye for staining cultured cells. In conclusion, almost all the synthesized heterocyclic compounds are able to stain cultured HeLa cell after fixing and give fluorescence at the sky blue region. This methodology will be readily applicable to the synthesis of various substituted pyranoquinoline derivatives for use as dye for staining cultured cell. Although compounds have a peak at 520-530 nm region in the emission spectrum, the compounds show red color fluorescence during staining, may be a due to shift in the peak area after binding.

Molecular modeling

The fluorescence, UV-Vis, and CD spectroscopic results were complemented with molecular modeling, in which TPQ was docked to BSA to determine the preferred binding site and the binding mode. Molecular docking technique has been applied to understand the binding modes of BSA-TPQ interaction [59, 60]. The 3D structure of BSA was obtained from Proteins Data Bank. The possible conformations of the BSA-TPQ complex were

calculated using Auto dock 4.0 program. Out of 10 conformers obtained, the conformer with the lowest binding free energy was used for further analysis. The best energy ranked model (**Fig. 9(a)**) revealed that the TPQ bound at the interface between two sub domains IIA and IIIA, which is located just above the entrance of the binding pocket of IIA. TPQ 2 molecule is surrounded by 10 amino acid residues within 5 Å: 5 hydrophobic residue (Leu122, Leu115, Phe133, Pro117, Ile181), 2 hydrophilic residues (Tyr160, Tyr137) and 4 ionic residues (Arg185, Glu125, Lys116, Lys136). Furthermore there is one hydrogen bond between the hydroxyl groups of TPQ 2 and the amino acid residue of Tyr 160 in chain A of BSA, Tyr160: OH: B-Lig1: N (**Fig. 9(b)**).

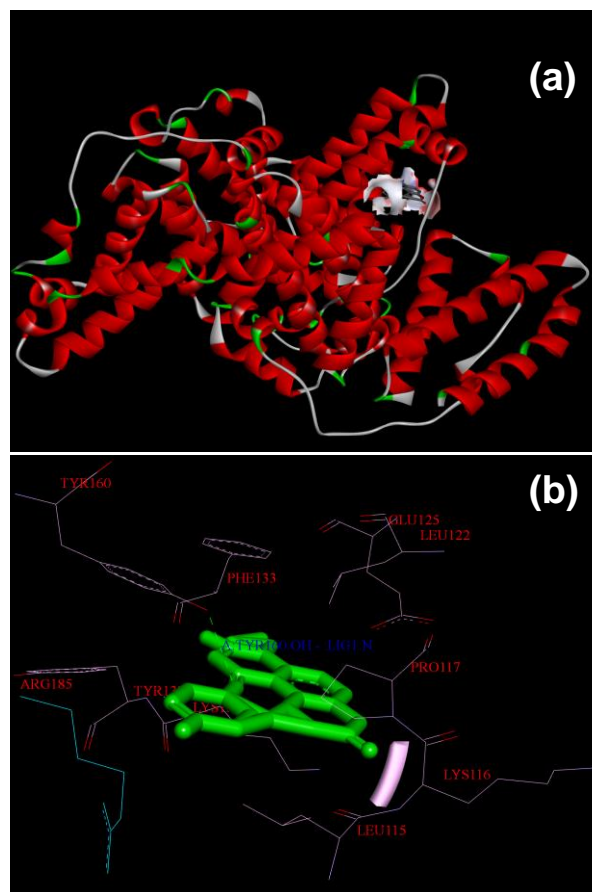


Fig. 9. Best conformation for TPQ 2 docked to BSA, (a) place of interaction of TPQ 2 and BSA and (b) The surrounding amino acid residues of BSA within 5 Å from TPQ 2 (green colored).

In case of TPQ 3, TPQ 4, TPQ 5 and TPQ 9 similar type of results were observed (S1). The formation of hydrogen bonds decreases the hydrophilicity and increases the hydrophobicity to stabilize the BSA-TPQ system [44]. Therefore, it can be concluded that the interaction between TPQ and BSA is dominated by hydrogen bonding and van der Waals interactions, which is in well agreement with the results of experimental binding mode study.

Conclusion

The binding study of drugs with proteins is of great importance in pharmacy, pharmacology and biochemistry. The interaction BSA with TPQ has been extensively

studied using absorption, fluorescence, and circular dichroism spectroscopic techniques. Experimental results confirmed that the quenching of the fluorescence emission from serum albumins by TPQ follows a dynamic quenching mechanism and TPQ bind to serum albumins with high affinity. The binding constants (K) and the apparent association (K_{app}) constants suggested that BSA has affinity towards synthesized sample TPQ. The binding of BSA-TPQ is mainly driven by van der Waals interactions and hydrogen bonding. The results of CD spectrum indicate that the secondary structure of BSA molecule changes in the presence of TPQ. The distance between the serum albumins and TPQ has been found to be <7 nm as calculated using FRET. The TPQ can be used as dyes for staining cultured cell. Furthermore, molecular docking study confirms the interaction between the TPQ and BSA and consistent with available investigational data.

Acknowledgements

SR is thankful to the Department of Science and Technology (New Delhi, India) for a DST INSPIRE fellowship (IF110421). S.P and T.G thank CSIR (New Delhi) for their fellowships.

Author contributions

Conceived the plan: SR, RS; Performed the experiments: SR; Data analysis: SR; Wrote the paper: SR, TKD, SP, TG, KCM (SR, TKD, SP, RKN, KCM are the initials of authors). Authors have no competing financial interests.

Reference

- Gao, H.; Lei, L.; Liu, J.; Kong, Q.; Chen, X.; Hu, Z. *J. Photochem. Photobiol. A: Chem.* **2004**, *167*, 213.
DOI: [10.1039/c0cs00136h](https://doi.org/10.1039/c0cs00136h)
- Silva, D.; Cortez, C. M.; Louro, S. R. W. *Spectrochim. Acta A*, **2004**, *60*, 1215.
DOI: [10.1016/j.saa.2003.08.003](https://doi.org/10.1016/j.saa.2003.08.003)
- Li, Y.; He, W.; Liu, J.; Sheng, F.; Hu, Z.; Chen, X. *Biochim. Biophys. Acta*, **2005**, *1722*, 15.
DOI: [10.1016/j.bbagen.2004.11.006](https://doi.org/10.1016/j.bbagen.2004.11.006)
- Wang, C.; Hu, Q.; Li, C.; Wang, Z.; Ma, J.; Zang, X. *Anal. Sci.*, **2007**, *23*, 429.
DOI: [10.2116/analsci.23.429](https://doi.org/10.2116/analsci.23.429)
- Mandeville, J. S.; Tajmir-Riahi, H. A. *Biomacromolecules*, **2010**, *11*, 465.
DOI: [10.1021/bm9011979](https://doi.org/10.1021/bm9011979)
- Jin, X. L.; Wei, X.; Qi, F. M.; Yu, S. S.; Zhou, B.; Bai, S. *Org. Biomol. Chem.*, **2012**, *10*, 3424-3431.
DOI: [10.1039/C2OB25237F](https://doi.org/10.1039/C2OB25237F)
- Jenekhe, S. A.; Lu, L.; Alam, M. M. *Macro molecules* **2001**, *34*, 7315.
DOI: [10.1021/ma0100448](https://doi.org/10.1021/ma0100448)
- Agrawal, A. K.; Jenekhe, S. A.; Vanher zeele, H.; Meth, J. S. *J. Phys. Chem.* **1992**, *96*, 2837.
DOI: [10.1021/j100186a011](https://doi.org/10.1021/j100186a011)
- Jegou, G.; Jenekhe, S. A. *Macromolecules* **2001**, *34*, 7926.
DOI: [10.1021/ma0111562](https://doi.org/10.1021/ma0111562)
- Lu, L.; Jenekhe, S. A. *Macromolecules* **2001**, *34*, 6249.
DOI: [10.1021/ma010086w](https://doi.org/10.1021/ma010086w)
- Saito, I.; Sando, S.; Nakatani, K. *Bioorg. Med. Chem.* **2001**, *9*, 2381.
DOI: [10.1016/S0968-0896\(01\)00160-2](https://doi.org/10.1016/S0968-0896(01)00160-2)
- Balasubramanian, M.; Keay, J. G. In *Comprehensive Heterocyclic Chemistry II*; Katritzky, A. R.; Rees, C. W.; Scriven, E. F. V. Eds.; Pergamon Press: Oxford, UK, **1996**; Vol. 5, pp 245.
- Cheng, X.-M.; Lee, C.; Klutchko, S.; Winters, T.; Reynolds, E. E.; Welch, K. M.; Flynn, M. A.; Doherty, A. M. *Bioorg. Med. Chem. Lett.* **1996**, *6*, 2999.
DOI: [10.1016/S0960-894X\(96\)00551-3](https://doi.org/10.1016/S0960-894X(96)00551-3)
- Anzini, M.; Cappelli, A.; Vomero, S.; Giorgi, G.; Langer, T.; Hamon, M.; Merahi, N.; Emerit, B. M.; Cagnotto, A.; Skorupska, M.; Mennini, T.; Pinto, J. C. *J. Med. Chem.* **1995**, *38*, 2692.
DOI: [10.1021/jm00014a021](https://doi.org/10.1021/jm00014a021)
- Giardina, G. A. M.; Sarau, H. M.; Farina, C.; Medhurst, A. D.; Grugni, M.; Raveglia, L. F.; Schmidt, D. B.; Rigolio, R.; Luttmann, M.; Vecchiotti, V.; Hay, D. W. P. *J. Med. Chem.* **1997**, *40*, 1794.
DOI: [10.1021/jm960818o](https://doi.org/10.1021/jm960818o)
- Ife, R. J.; Brown, T. H.; Keeling, D. J.; Leach, C. A.; Meeson, M. L.; Parsons, M. E.; Reavill, D. R.; Theobald, C. J.; Wiggall, K. J. *J. Med. Chem.* **1992**, *35*, 3413.
DOI: [10.1021/jm00096a018](https://doi.org/10.1021/jm00096a018)
- Chen, S.-F.; Papp, L. M.; Ardecky, R. J.; Rao, G. V.; Hesson, D. P.; Forbes, M.; Desxter, D. L. *Biochem. Pharmacol.* **1990**, *40*, 709.
DOI: [10.1016/0006-2952\(90\)90305-5](https://doi.org/10.1016/0006-2952(90)90305-5)
- Nestrova, I. N.; Alekseeva, L. M.; Andreeva, N. I.; Glovira, S. M.; Granic, V. G. *Khim. Farm. Zh.* **1995**, *29*, 31 (Russ); *Chem. Abstr.* **1996**, *124*, 117128t.
- Yamada, N.; Kadowaki, S.; Takahashi, K.; Umezu, K. *Biochem. Pharmacol.* **1992**, *44*, 1211.
DOI: [10.1016/0006-2952\(92\)90387-X](https://doi.org/10.1016/0006-2952(92)90387-X)
- Faber, K.; Strueckler, H.; Kappe, T. J. *Heterocycl. Chem.* **1984**, *21*, 1177.
DOI: [10.1002/jhet.5570210450](https://doi.org/10.1002/jhet.5570210450)
- Akhmed Khodzhaeva, Kh. S.; Besonova, I. A. *Dokl. Akad. Nauk. Uzh. SSR* **1982**, *34-36* (Russ); *Chem. Abstr.* **1983**, *98*, 83727q.
- Mohamed, E. A. *Chem. Pap.* **1984**, *48*, 261. *Chem. Abstr.* **1995**, *123*, 9315x.
- Marco, J. L.; Carreiras, M. C. *J. Med. Chem.* **2003**, *6*, 518.
- Puricelli, L.; Innocenti, G.; Delle Monache, G.; Caniato, R.; Filippini, R.; Cappelletti, E. M. *Nat. Prod. Lett.* **2002**, *16*, 95.
DOI: [10.1080/10575630290019985](https://doi.org/10.1080/10575630290019985)
- Corral, R. A.; Orazi, O. O. *Tetrahedron Lett.* **1967**, *7*, 583.
DOI: [10.1016/S0040-4039\(00\)90553-7](https://doi.org/10.1016/S0040-4039(00)90553-7)
- Sekar, M.; Rejendra Prasad, K. J. *J. Nat. Prod.* **1998**, *61*, 294.
DOI: [10.1021/np970005i](https://doi.org/10.1021/np970005i)
- Majumdar, K. C.; Ponra, S.; Ghosh, T. *Tetrahedron Letters*, **2013**, *54*, 5586-5590.
DOI: [Doi: 10.1016/j.tetlet.2013.07.163](https://doi.org/10.1016/j.tetlet.2013.07.163)
- Ghosh, U.; Bhattacharyya, N. P. *Mol. Cell Biochem.* **2009**, *320*, 15-23.
DOI: [10.1007/s11010-008-9894-2](https://doi.org/10.1007/s11010-008-9894-2)
- Mukherjee, S.; Basu, C.; Chowdhury, S.; Chattopadhyay, A. P.; Ghorai, A.; Ghosh, U.; Stoeckli-Evans, H. *Inorg. Chim. Acta*, **2010**, *363*, 2752-2761.
DOI: [10.1016/j.ica.2010.04.02](https://doi.org/10.1016/j.ica.2010.04.02)
- Ghosh, K.; Sarkar, A. R.; Ghorai, A.; Ghosh, U. *New J. Chem.* **2012**, *36*, 1231.
DOI: [10.1039/C2NJ21024J](https://doi.org/10.1039/C2NJ21024J)
- Roy, S.; Sadhukhan, R.; Ghosh, U.; Das, T. K. *Spectrochimica Acta Part A*, **2015**, *141*, 176-184.
DOI: [10.1016/j.saa.2015.01.041](https://doi.org/10.1016/j.saa.2015.01.041)
- Bi, S.; Song, D.; Tian, Y.; Zhou, X.; Liu, Z.; Zhang, H. *Spectrochim. Acta A*, **2005**, *61*, 629-636.
DOI: [10.1016/j.saa.2004.05.028](https://doi.org/10.1016/j.saa.2004.05.028)
- Stephanos, J. J. *J. Inorg. Biochem.* **1996**, *62*, 155-169. ISSN: 0162-0134.
- Marty, R.; Nsoukpoe-Kossi, N. C.; Charbonneau, D.; Weinert, C. M.; Kreplak, L.; Tajmir-Riahi, H. A. *Nucleic Acids Res.* **2009**, *37*, 849-857.
DOI: [10.1093/nar/gkn1003](https://doi.org/10.1093/nar/gkn1003)
- Wang, C. X.; Yan, F. F.; Zhang, Y. X.; Ye, L. *J. Photochem. Photobiol. A*, **2007**, *192*, 23-28.
DOI: [10.1016/j.jphotochem.2007.04.032](https://doi.org/10.1016/j.jphotochem.2007.04.032)
- Yi, P. G.; Shang, Z. C.; Yu, Q. S.; Shao, S.; Lin, R. S. *Acta. Chim. Sin.* **2000**, *58*, 1649-1653.
ISSN: 0567-7351
- Gao, D. J.; Tian, Y.; Bi, S. Y.; Chen, Y. H.; Yu, A. M.; Zhang, H. Q. *Spectrochim. Acta A*, **2005**, *62*, 1203-1208.
DOI: [10.1016/j.saa.2005.04.026](https://doi.org/10.1016/j.saa.2005.04.026)
- Ware, W. R. *J. Phys. Chem.* **1962**, *66*, 455-458.
DOI: [10.1021/j100809a020](https://doi.org/10.1021/j100809a020)
- Li, J. C.; Li, N.; Wu, Q. H.; Wang, Z.; Ma, J. J.; Wang, C.; Zhang, L. J. *J. Mol. Struct.* **2007**, *833*, 184-188.
DOI: [10.1016/j.molstruc.2006.09.019](https://doi.org/10.1016/j.molstruc.2006.09.019)
- Roy, S.; Das, T. K. *J. Nanosci. Nanotechnol.* **2014**, *14*, 4899.
DOI: [10.1166/jnn.2014.9508](https://doi.org/10.1166/jnn.2014.9508)
- Cao, H.; Liu, Q. *J. Solution Chem.* **2009**, *38*, 1071-1077.
DOI: [10.1007/s10953-009-9430-3](https://doi.org/10.1007/s10953-009-9430-3)

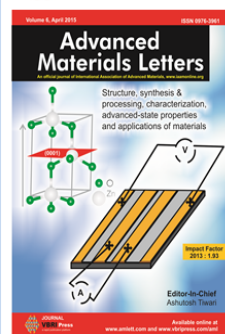
42. Kandagal, P. B.; Ashoka, S.; Seetharamappa, J.; Shaikh, S. M. T.; Jadedgoud, Y.; Ijare, O. B. *J Pharm. Biomed. Anal.* **41**, **2006**, 393-399.
DOI: [10.1016/j.jpba.2005.11.037](https://doi.org/10.1016/j.jpba.2005.11.037)
43. Ross, D. P.; Subramanian, S. *Biochemistry*, **1981**, *20*, 3096-3102.
DOI: [10.1021/bi00514a017](https://doi.org/10.1021/bi00514a017)
44. Neméthy, G.; Scheraga, H. A. *J. Phys. Chem.* **1962**, *66*, 1773-1789.
DOI: [10.1021/j100816a004](https://doi.org/10.1021/j100816a004)
45. Roy, S.; Das, T. K. *Nanosci. Nanotechnol. Lett.* **2014**, *6*, 547-554.
DOI: [10.1166/nnl.2014.1852](https://doi.org/10.1166/nnl.2014.1852)
46. Roy, S.; Das, T. K. *Adv. Sci Eng. Med.* **2014**, *6*, 1105-1110.
DOI: [10.1166/asem.2014.1617](https://doi.org/10.1166/asem.2014.1617)
47. Hu, Y.-J.; Liu, Y.; Pi, Z.-B.; Qu, S.-S. *Bioorg. Med. Chem.* **2005**, *13*, 6609-6614.
DOI: [10.1016/j.bmc.2005.07.039](https://doi.org/10.1016/j.bmc.2005.07.039)
48. Fuller C. W.; Miller, J. N. *Proc. Anal. Div. Chem. Soc.*, **1979**, *16*, 199.
DOI: [10.1039/AD9791600199](https://doi.org/10.1039/AD9791600199)
49. Zhang, Y.; Zhou, B.; Liu, Y.; Zhou, C.; Ding, X.; Liu, Y. *J. Fluoresc.* **2008**, *18*, 109-118.
DOI: [10.1007/s10895-007-0247-4](https://doi.org/10.1007/s10895-007-0247-4)
50. Kelly, S. M.; Tess, T. J.; Price, N. C. *Biochim. Biophys. Acta*, **2005**, *1751*, 119-139.
DOI: [10.1016/j.bbapap.2005.06.005](https://doi.org/10.1016/j.bbapap.2005.06.005)
51. Kandagal, P. B.; Seetharamappa, J.; Ashoka, S.; Shaikh, S. M. T.; Manjunatha, D. H. *Int. J. Biol. Macromol.* **2006**, *39*, 234-239.
DOI: [10.1016/j.jpba.2005.11.037](https://doi.org/10.1016/j.jpba.2005.11.037)
52. Cheng, X. X.; Liu, Y.; Zhou, B.; Xiao, X. H.; Liu, Y. *Spectrochim. Acta A*, **2009**, *72*, 922-928.
DOI: [10.1016/j.saa.2008.12.003](https://doi.org/10.1016/j.saa.2008.12.003)
53. Kang, J.; Liu, Y.; Xia Xie, M.; Li, S.; Jiang, M.; Wang, Y. D. *Biochim. Biophys. Acta*, **2004**, *1674*, 205-214.
DOI: [10.1016/j.bbagen.2004.06.021](https://doi.org/10.1016/j.bbagen.2004.06.021)
54. Yang, M. M.; Yang, P.; Zhang, L. W. *Chin. Sci. Bull.* **1994**, *39*, 734-739. ISSN: 1001-6538 (Print), ISSN: 1861-9541 (online).
55. Förster, T. in: O. Sinanoglu (Ed.), *Modern Quantum Chemistry*, Academic Press, New York, **1996**.
56. Shang, Z. C.; Yi, P. G.; Yu, Q. S.; Lin, R. S. *Acta Phys. Chim. Sin.* **2001**, *17*, 48-52.
DOI: [10.3866/PKU.WHXB20010110](https://doi.org/10.3866/PKU.WHXB20010110)
57. Zhang, H. X.; Huang, X.; Mei, P.; Li, K. H.; Yan, C. N. *J. Fluoresc.* **2006**, *16*, 287-294.
DOI: [10.1007/s10895-006-0087-7](https://doi.org/10.1007/s10895-006-0087-7)
58. Ni, Y. N.; Su, S. J.; Kokot, S. *Spectrochim. Acta A*, **2010**, *75*, 547-552.
DOI: [10.1016/j.saa.2009.11.014](https://doi.org/10.1016/j.saa.2009.11.014)
59. Gao, W. H.; Li, N.; Chen, Y. W.; Xu, Y.; Lin, Y.; Yin, Y.; Hu, Z. J. *Mol Struct.* **2010**, *983*, 133-140.
DOI: [10.1016/j.molstruc.2010.08.042](https://doi.org/10.1016/j.molstruc.2010.08.042)
60. Paal, K.; Shkarupin, A.; Beckford, L. *Bioorg. Med Chem.* **2007**, *15*, 1323-1329.
DOI: [10.1016/j.molstruc.2010.08.042](https://doi.org/10.1016/j.molstruc.2010.08.042)

Advanced Materials Letters

Copyright © VBRI Press AB, Sweden
www.vbripress.com

Publish your article in this journal

Advanced Materials Letters is an official international journal of International Association of Advanced Materials (IAAM, www.iaamonline.org) published by VBRI Press AB, Sweden monthly. The journal is intended to provide top-quality peer-review articles in the fascinating field of materials science and technology particularly in the area of structure, synthesis and processing, characterisation, advanced-state properties, and application of materials. All published articles are indexed in various databases and are available download for free. The manuscript management system is completely electronic and has fast and fair peer-review process. The journal includes review article, research article, notes, letter to editor and short communications.



Supporting information

Table 1. The Stern-Volmer constants and quenching constants of BSA by STP at varying temperature.

Compound	Temperature (K)	K_{SV} (L/mol) $\times 10^2$	K_q (L/mol/S) $\times 10^{-6}$	R^a
TPQ2	293	3.52	3.52	0.9985
TPQ3	293	3.36	3.36	0.9982
TPQ4	293	4.88	4.88	0.9968
TPQ5	293	1.54	1.54	0.9963
TPQ9	293	2.42	2.42	0.9984
TPQ2	300	4.20	4.20	0.9989
TPQ3	300	3.50	3.50	0.9992
TPQ4	300	4.89	4.89	0.9984
TPQ5	300	1.51	1.51	0.9985
TPQ9	300	2.97	2.97	0.9984
TPQ2	308	4.59	4.59	0.9977
TPQ3	308	4.01	4.01	0.9986
TPQ4	308	4.92	4.92	0.9959
TPQ5	308	1.99	1.99	0.9960
TPQ9	308	3.22	3.22	0.9998
TPQ2	315	4.92	4.92	0.9989
TPQ3	315	4.96	4.96	0.9965
TPQ4	315	4.70	4.70	0.9914
TPQ5	315	2.32	2.32	0.9974
TPQ9	315	3.30	3.30	0.9974

^aCorrelation coefficient.

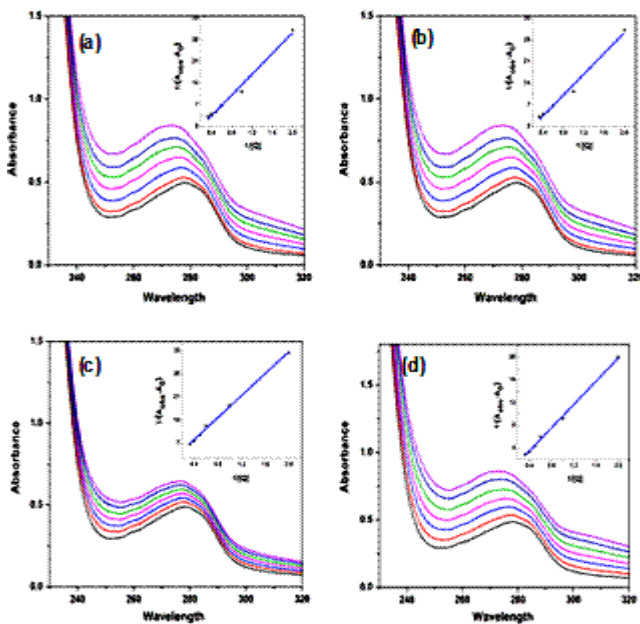


Fig. S1. (color online) Absorption spectra of BSA (1 μ M) in presence of TPQ 3, TPQ 4, TPQ 5 and TPQ 9 [a, b, c and d respectively] (1-7): (0 to 30 μ M), inset showing calculation of K_{app} of BSA-TPQ complex; $1/(A_{obs}-A_0)$ vs $1/[TPQ]$ plot.

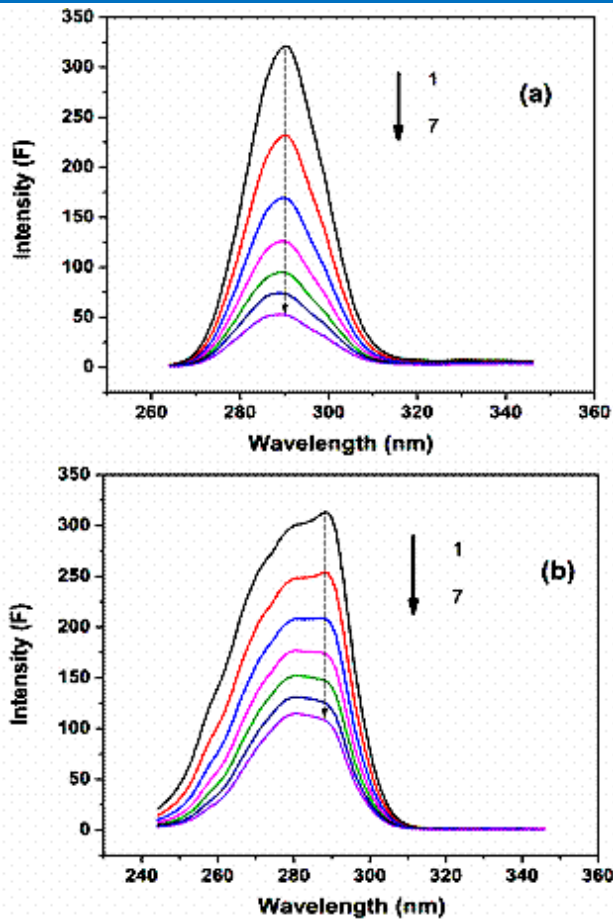


Fig. 5. Synchronous fluorescence spectra of BSA in presence of TPQ 2 while the $\Delta\lambda=15$ nm (a) and $\Delta\lambda=60$ nm (b).

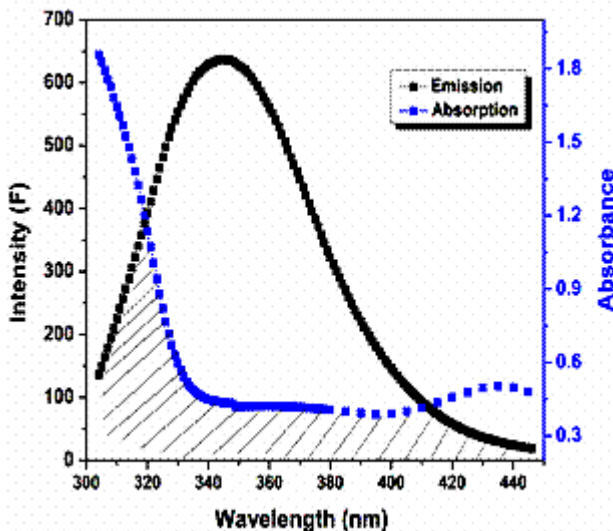


Fig. 7. Overlap plot of the fluorescence emission spectrum of BSA (1 μ M) and the UV absorption spectrum of TPQ 2 (1 mM).

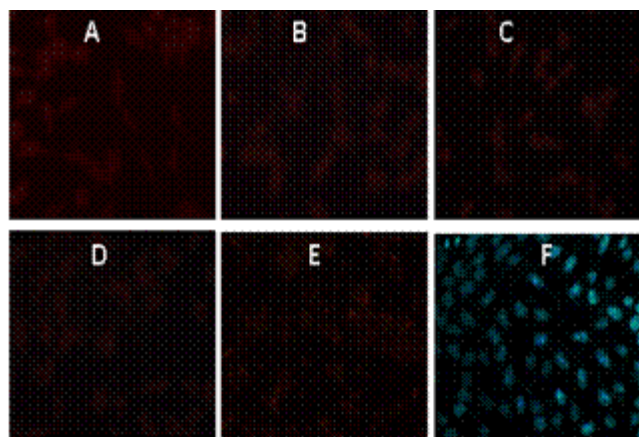
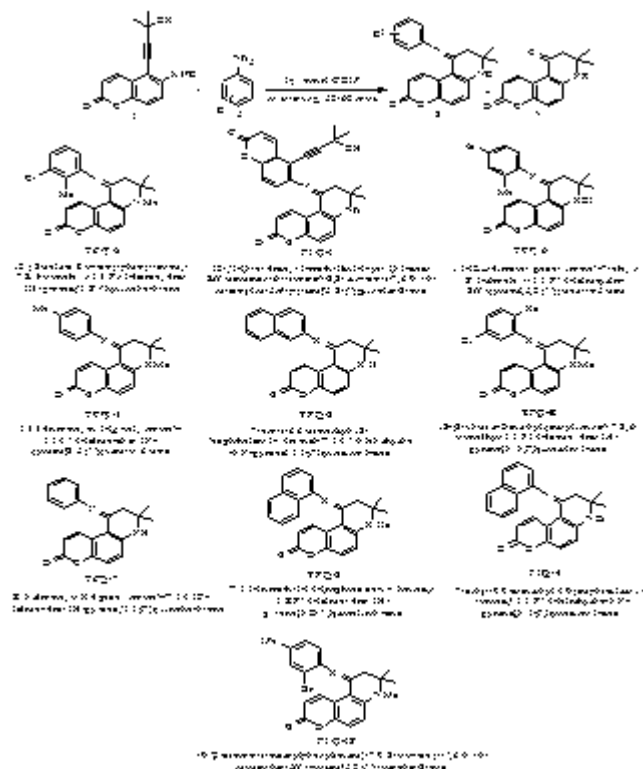


Fig. 8. HeLa cells stained with Hoechst dye and synthetic compounds. In figure- (F), Hoechst dye, (A-E), compound TPQ 2-5, TPQ 9.

Table 4. The energy transfer parameters between TPQ and BSA.

System	$J \times \text{cm}^3 \times \text{L/mol}$	E	R_0 (nm)	R (nm)
BSA-TPQ2	2.82×10^{-15}	0.11	2.07	2.93
BSA-TPQ3	2.66×10^{-15}	0.112	2.05	2.89
BSA-TPQ4	1.91×10^{-15}	0.127	1.94	2.67
BSA-TPQ5	2.03×10^{-15}	0.073	1.96	2.99
BSA-TPQ9	2.31×10^{-15}	0.085	1.999	2.97

^a Correlation coefficient.



Scheme 1: Synthesized pyranoquinoline derivatives.